

Electronic properties and Fermi surfaces $MgCN_3$ and related intermetallics

I.R. Shein, N.I. Medvedeva, A.L. Ivanovskii

Institute of Solid State Chemistry, Ural Branch of the Russian Academy of Sciences, 620219
Ekaterinburg, Russia

Abstract

The band structure of the new perovskite-like superconductor $MgCN_3$ was studied by the self-consistent FP-LMTO method. The superconducting properties of $MgCN_3$ are associated with an intensive peak in the density of $Ni3d$ states near the Fermi level. The absence of superconductivity for nonstoichiometric compositions $MgC_{1-x}N_3$ is due to the transition of the system to the magnetic state. The possibility of superconductivity was discussed for intermetallics $ScBN_3$, $InBN_3$, $MgBCO_3$ and $MgCCu_3$ which are isostructural with $MgCN_3$.

Typeset using REVTEX

The discovery (2001 [1]) of the superconducting transition ($T_c = 39$ K) for intermetallic MgB_2 gave impetus to wide search for novel superconductors (SC) among related compounds which is carried out now in three basic directions. The first direction is to the expansion of the class of MgB_2 -based SC by doping it or by creating superstructures [2]. In the second direction SC candidates are looked for among binary or multicomponent phases with elements of structural or chemical similarity with MgB_2 . As a result, critical transitions were found for ZrB_2 (5.5 K [3]), TaB_2 (9.5 K [4]), ReB (4.7 K [5]), the new beryllium boride phase (0.72 K, the composition $BeB_{2.75}$, the unit cell containing 110.5 atoms [6]). The development of the third direction was initiated by the observation [7] of superconductivity in the ternary intermetallic, viz. the perovskite-like $MgCN_b$ ($T_c = 8$ K). Some circumstances make the finding [7] especially interesting.

1. The high-symmetry structure of $MgCN_b$ (space group $Pm\bar{3}m$) is a favourable factor for superconductivity. However, all known to date SC perovskites contain oxygen atoms in 3C-type sites (0; 1/2; 1/2), the electron-hole states of which play the basic role in the formation of superconductivity [8]. For $MgCN_b$, those sites are occupied by Ni atoms, i.e. the mechanism of SC should be of a fundamentally different nature.
2. The majority of known "non-oxide" perovskite-like phases $MX M_3^0$ (the so-called antiperovskites, where $M = Zn, Al, Ga, In, Sn; M' = Mn, Fe; X = C, N$) exhibit ferro-, antiferromagnetic properties, or have a more complicated spin ordering [9]. Hence, in the series of structural analogs, $MgCN_b$ can be considered as a "boundary" phase between perovskite-like SC (oxides) and magnetics (non-oxygen perovskites).
3. The closest chemical analogs of $MgCN_b$ superconducting borocarbides of intermetallics (BCI) of the general composition LnM_2B_2C . They also include nickel-containing phases $LuNi_2B_2C$ ($T_c = 16$ K), YNi_2B_2C ($T_c = 15.6$ K). However, as distinct from $MgCN_b$, BCI (i) are magnetic superconductors, (ii) they have a quasi-two-dimensional structure composed of $(Lu, Y)C$ layers and NiB_4 tetrahedra [10], and (iii) the content of Ni (magnetic metal) in BCI is considerably smaller (35.6 – 48.9 at.%) than in $MgCN_b$ (82.9 at.%).

The first investigations of some properties of $MgCN_b$, namely the critical field (H_{c2}), Hall coefficient, other electrophysical characteristics [11–14], made it possible to assign $MgCN_b$ to "conventional" superconductors of the II-nd type with an electron-phonon type of interactions. In that case the critical temperature can be estimated from the Mullen formula $T_c = \langle w \rangle \exp(f(\lambda))$, where $\langle w \rangle$ is an averaged phonon frequency, λ is the electron-phonon interaction constant $\lambda = N(E_F) \langle I^2 \rangle$, where $N(E_F)$ is the density of states on a Fermi level and $\langle I^2 \rangle$ is average square of a matrix device an electron-phonon interaction. Therefore the information on the band structure plays a significant role both for the interpretation of superconducting (and other) properties of $MgCN_b$ and for the quest of possible SC analogs. In this paper we present the results of investigations of the band structure of the new SC $MgCN_b$, discuss the effect of C vacancies (nonstoichiometry in carbon sublattice) on its electronic properties and analyze the peculiarities of electronic and magnetic states for related perovskite-like alloys ($ScBN_b$, $InBN_b$, $MgBCO_3$ and $MgCCu_3$) as probable superconductors. The self-consistent spin-polarized full-potential linear muffin-tin orbital (FP-LMTO) method [15] in the framework of local (spin) density approximation (LDA) with relativistic effects according to the scheme [16] and with an exchange-correlation potential proposed in [17] was used in the calculations. In the structure of $MgCN_b$, atoms occupy the following positions: 3Ni (0; 1/2; 1/2), Mg (0; 0; 0), C (1/2; 1/2; 1/2). Their coordination polyhedra

(CP) are NiC_2Mg_4 and $[\text{CN}]$ octahedra for Ni and C and the cubooctahedron $[\text{MgNi}_2]$ for magnesium. The theoretical equilibrium lattice parameter of MgCNi_3 (3.721 Å) defined by minimization of the total energy appeared to be in good agreement with the experimental value 3.8066 Å (for $\text{MgC}_{0.96}\text{Ni}_3$ with $T = 0$ K) [18].

The band structure for MgCNi_3 (Figs. 1–3) are a good agreement with the calculation of authors [19]. The most important feature of the MgCNi_3 spectrum is the presence of an intensive DOS peak near the E_F associated with the quasiplanar antibonding Ni3d bands (in the directions $X\text{-M}$ and $M\text{-}$ of the Brillouin zone), see Fig. 1. The Ni (E_F) is located on the high-energy slope of the peak. The value of Ni (E_F) is 4.57 states/eV, which accords well the full-potential FLAPW calculation (4.99 states/eV [20]). The expansion of Ni (E_F) into orbital components ($N_i(E_F)$) shows (Table 1) that the maximum contribution to Ni (E_F) (4.04 state/eV, or 88.2%) is due to the Ni3d states. The contributions of C 2s,p and Mg 3s,p,d states to Ni (E_F) are 0.23 (5.08%) and 0.14 states/eV (3.03%) respectively. The Stoner parameter $S = N(E_F)I_{\text{ex}}$ (I_{ex} – exchange integral) is 0.55, the magnetic moments on atoms are absent. The upper of the two antibonding Ni3d bands, which has a more pronounced dispersion, is responsible for the electronic type of the Fermi surface (Fig. 3) having the form of spheroids near the Γ point and small sheets along the boundaries and angles of the Brillouin zone. The latter Ni3d band produces clover-type sheets centered in the X point and cigar-like figures along the -R direction.

To compare individual interatomic bonds we calculated used by the tight-binding band method the crystal orbital overlap populations (COOP) of MgCNi_3 and ScBNi_3 . The corresponding values for MgCNi_3 were 0.298 (Ni–C), 0.027 (Ni–Ni) and 0.039 e/bond (Ni–Mg). So, the Ni–C bonds (in the $[\text{CN}]$ CP, Fig. 4) are the dominant interatomic interactions in MgCNi_3 . The C–Mg bonding is negligibly small (0.002 e/bond). For ScBNi_3 , these values are 0.338 (Sc–B), 0.050 (Ni–Ni), 0.033 (Ni–Sc) and 0.005 e/bond (B–Sc). These results make it possible to explain the data [13] on temperature dependence of the Debye–Waller factor (DW F) for atoms in MgCNi_3 . The minimum (isotropic) temperature factor of carbon corresponds to its most bonding (and high-symmetry – in the center of Ni_6 octahedron) state in the crystal, whereas for Ni the DW F has a greater value and is anisotropic: in the CP of Ni (NiC_2Mg_4 octahedra) the COOP of different-type (Ni–C and Ni–Mg) bonds differ by an order of magnitude. The observed minimum mean-square displacements (U_{11}) of nickel correspond to the directions of the strongest Ni–C bonds.

Based on Fig. 2, in the framework of the rigid-band model it can be expected that the introduction of electronic or hole dopants into MgCNi_3 will bring about an increase or decrease in Ni (E_F) respectively. In the first case, the SC of the system is expected to worsen. Doping by holes, which promises an increase in Ni (E_F) and is a favorable factor for a rise in T_c , can, however, cause a transition of the system to the magnetic state with loss of SC. A similar band structure (an intensive near-Fermi peak of metallic states generally indicating the instability of the nonmagnetic state of the system) is realized for the superconducting BC1 and determines the formation of atomic magnetic moments (MM) [4].

We have carried out the calculations of the system simulating these modifications. The effect of a decrease in the occupation of energy bands was viewed as a result of the presence of vacancies in the C–sublattice of MgCNi_3 (hypothetical perovskite MgENi_3 with "empty" C sublattice, E – vacancy) or the Ni \rightarrow Co substitution (MgGCo_3). Electron concentration growth was simulated using the MgGCo_3 phase as an example. In addition, stable boron–

containing phases isostructural and isoelectronic with $MgCN_3$, namely $ScBN_3$ and $InBN_3$ with lattice parameters given in [21], were considered for the first time as possible SC. For the "nonstoichiometric" antiperovskite it was found that $MgEN_3$ is in the magnetic state, atom M being 0.44 and -0.05 B for Mg and N atoms respectively. An analogous result was obtained also for $InEN_3$: M are 0.20 B for N and -0.01 B for In atoms. Hence, the experimentally noticed [7] condition of obtaining the superconducting $MgCN_3$ as a phase of strictly stoichiometric composition $MgC_{1-x}N_3$ samples ($x > 0.1$) lose SC) is primarily by the peculiarities of its electronic structure.

The ground state of the antiperovskite $MgCCo_3$ appears from calculations to be magnetic, M of atoms being 0.36 for Co and -0.05 B for Mg . For $MgCCu_3$, we found that (i) the electron concentration growth results in the filling of antibonding bands, Fig. 1, and (ii) $N(E_F)$ with dominating delocalized sp states decreases by more than an order as compared to $MgCN_3$, Fig. 3. The data obtained allow us to explain the changes in the superconducting properties of $MgCN_3$ when the N sublattice is doped with 3d metals. It is known that the critical transition temperature for $MgCN_{3-x}M_x$ alloys ($M = Mn, Co, Cu$) [13, 14] drops if (i) the concentration of dopants increases or (ii) their atomic number diminishes ($Co \rightarrow Mn$). It is seen from the dependence between T_c and the concentration of copper that T_c decreases progressive in the limits $0 < x < 0.1$. Partial substitution of cobalt atoms for nickel leads to disappearance of superconductivity already for $x = 0.03$. The effect of superconductivity suppression strengthens for $Ni \rightarrow Mn$ substitution. According to calculated data, the nature of the above effect differs essentially for different dopants. For alloys with substituted Mn and Co , this is due to spin fluctuations; as for Cu , the reason is with the growth of the total electron concentration in the system and an abrupt decrease in $N(E_F)$. The results of calculations of boron-containing antiperovskites $ScBN_3$, $InBN_3$ are given in Figs. 1-4 and Table 1. Charge density for $MgCN_3$ and $ScBN_3$ (Fig. 4) show that covalent overlapping of Sc - B bonds is stronger than of Mg - C bonds, which completely coincides with the presented above data obtained by us in the framework of the tight-binding band theory. In going from $MgCN_3$, $ScBN_3$ and $InBN_3$ the Fermi level shifts to the high-energy region of the $Ni3d$ peak, and $N(E_F)$ decreases essentially. In this series of compounds, one of the antibonding bands lowers relative to the Fermi level along the M - direction and shifts upwards in the point X . In the M point, it shifts upwards, and in the direction $-R$ goes below the Fermi level. These changes in the band structure lead to the modification of the Fermi surface. Electronic-type sphere-like surfaces near the point undergo insignificant changes. The quasi-cylindrical electronic surface along the BZ edges increases in this series. No hole cigar-like figures along the $-R$ direction are present for $ScBN_3$ and $InBN_3$, and clover-type sheets on the faces of the BZ centered in the X point increase for $ScBN_3$ and degenerate in a spheroid for $InBN_3$. Thus, the Fermi surface topology for the considered compounds preserves the basic features of the superconducting $MgCN_3$. Fig. 3 also displays the Fermi surface for $MgCCu_3$. For this compound, the shift of the Fermi level results in a qualitatively different topology: neither electronic- nor hole-type surfaces are present in the vicinity of points M and X .

This double substitution causes changes in the electronic structure of the above isoelectronic system s, which may be expected to exhibit superconducting properties if doped with a small quantity of holes. The most probable ways are introduction of B vacancies (nonstoichiometry in boron sublattice, especially as for $InBN_3$ this possibility is known from experiment

[21]) or partial replacement of Sc by I, II group atoms. Doping of the Ni sublattice with magnetic impurities (Co, Mn) can be more problematic because of magnetic instability. Thus, the band structure of the new perovskite-like superconductor MgCNi₃ has been examined. Its superconducting properties are associated with the presence of the intensive Ni3d DOS peak near the Fermi level. Impairment of SC characteristics of MgCNi₃ doped with holes MgC_{1-x}Ni₃ compositions or with Co, Mn, is explained by the transition of the system to the magnetic state. The impairment of SC as a result of electron doping (alloys MgC_{1-x}Cu₃) is due to the filling of antibonding states and the abrupt decrease in N(E_F). It is pointed out that stoichiometric antiperovskites ScBNi₃ and InBNi₃ may exhibit superconducting properties.

REFERENCES

- [1] J. Nagamatsu, N. Nakagawa, T. M uranaka, Y. Zenitaniets., J. Akimoto Nature, 410, 63 (2001).
- [2] N. M edvedeva, U. E. M edvedeva, A. L. Ivanovskii etc., Letter in JETP, 73, 378 (2001).
- [3] V. A. Gasparov, N. S. Sidorov and M. P. Kulakov, cond-mat/0104323 (2001).
- [4] D. Kaczorowski, J. Klamut and A. Zaleski, cond-mat/0104479 (2001).
- [5] G. K. Strukova, V. F. Degt'yareva, D. V. Shirkun etc., cond-mat/0105293 (2001).
- [6] D. Young, P. Adams, J. Chan etc., cond-mat/0104063 (2001).
- [7] T. He, Q. Huang, A. P. Ramirez etc., cond-mat/0103296 (2001).
- [8] A. Taraphder, R. Pandit, H. R. Krishnamurthy and T. V. Ramakrishnan, Int. J. Mod. Phys., B 10, 863 (1998).
- [9] A. L. Ivanovskii, Successes of chemistry (Rus), 64, 499 (1995).
- [10] A. L. Ivanovskii, Successes of chemistry (Rus), 67, 493 (1998).
- [11] S. Y. Li, R. Fan, X. H. Chen etc., cond-mat/0104554 (2001).
- [12] Z. Q. Mao, M. M. Rosario, R. Nelson etc., cond-mat/0105280 (2001).
- [13] M. A. Hayward, M. K. Haas, T. He etc., cond-mat/0104541 (2001).
- [14] Z. A. Ren, G. C. Che, S. L. Jia etc., cond-mat/0105366 (2001).
- [15] M. ethfessel, Scheer M. Physica B, 172, 175 (1991).
- [16] Savrasov S. Y. Phys. Rev., B 54, 16470 (1996).
- [17] Vosko S. H., Wilk L., Nusair M. Canadian J. Phys., 58, 1200 (1980).
- [18] Q. Huang, T. He, K. A. Regan etc., cond-mat/0105240 (2001).
- [19] J. H. Shim and B. I. Min, cond-mat/0105418 (2001).
- [20] J. D. Singh and I. I. Mazin, cond-mat/0105577 (2001).
- [21] A. P. Kusma, Crystal chemistry of borides (Rus), L'vov, "Vyshashkola", 1983.

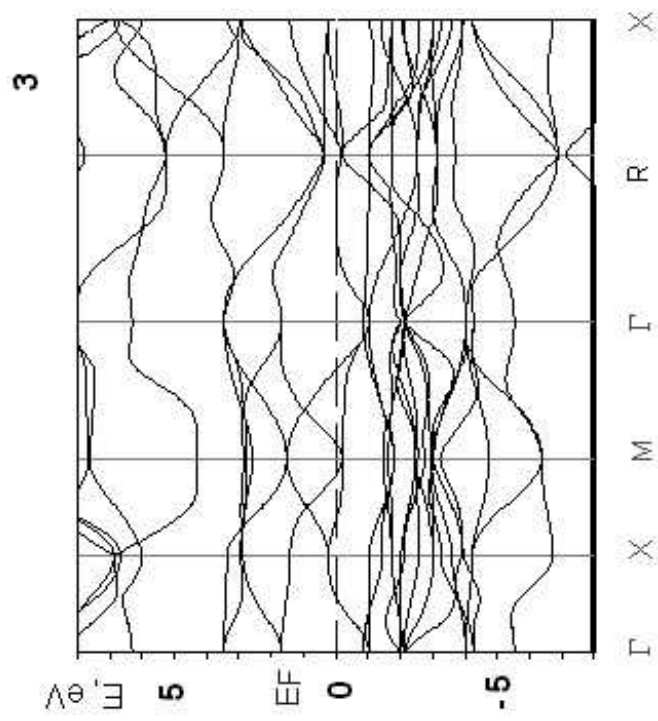
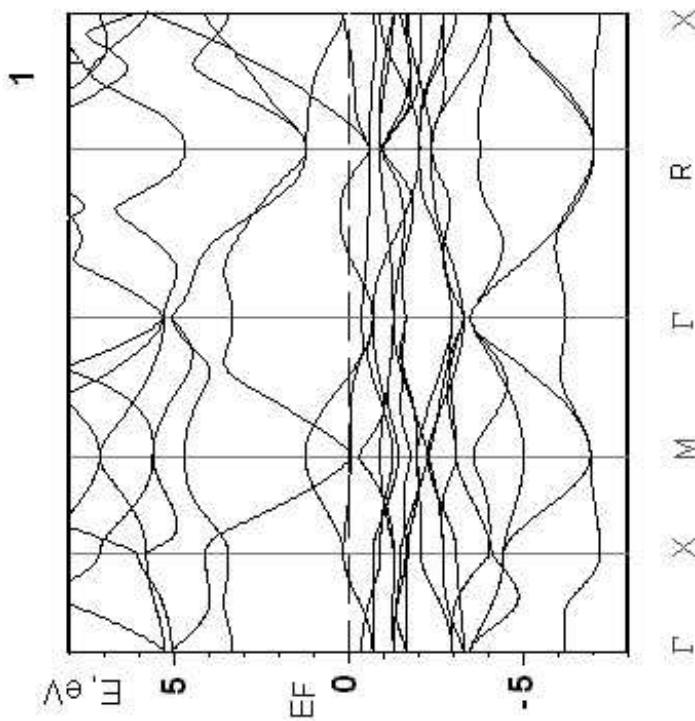
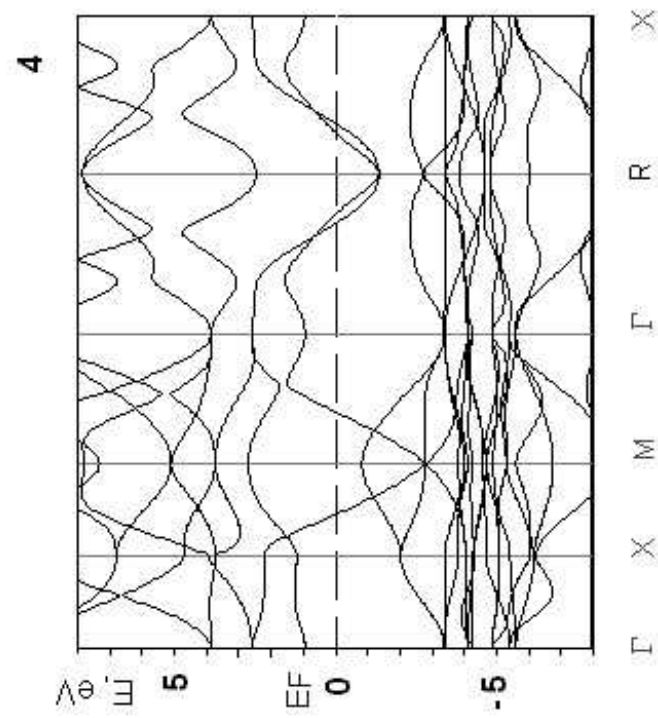
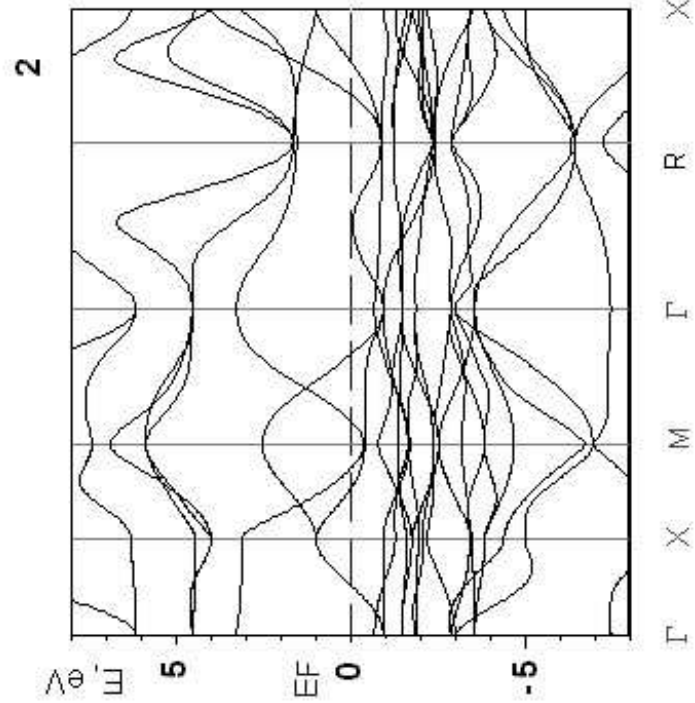
FIGURES:

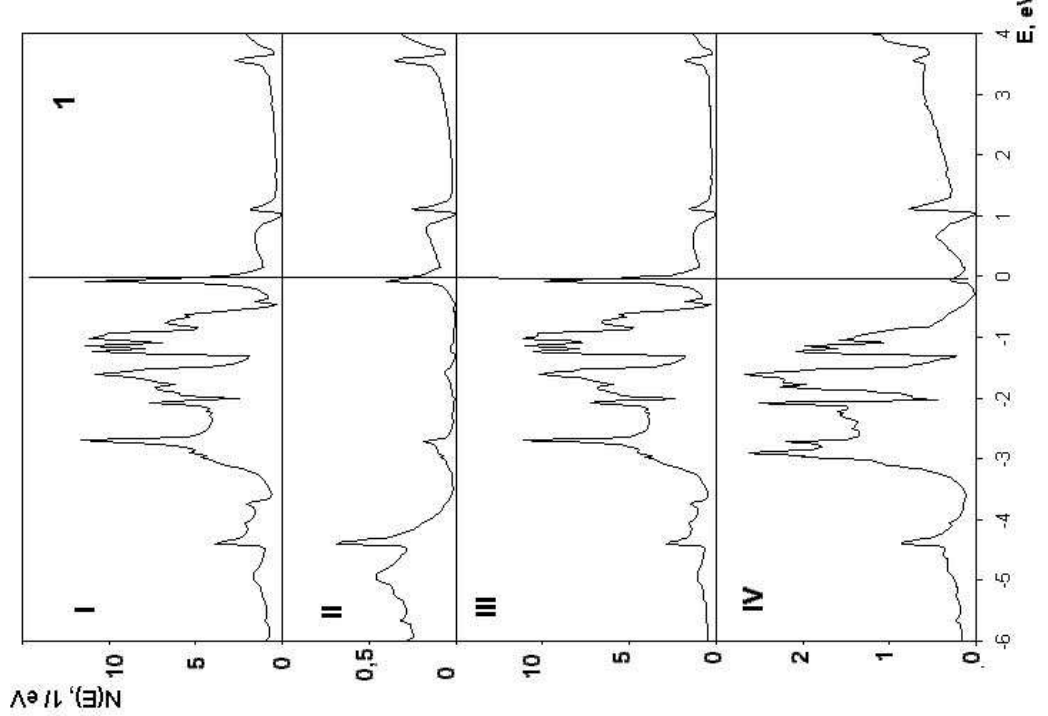
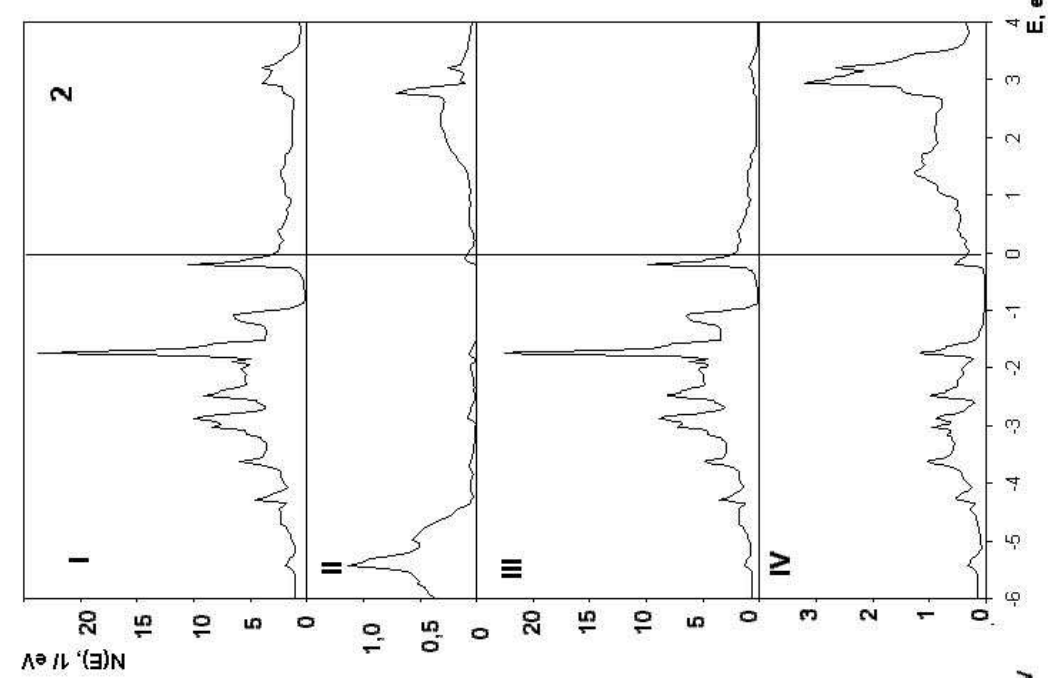
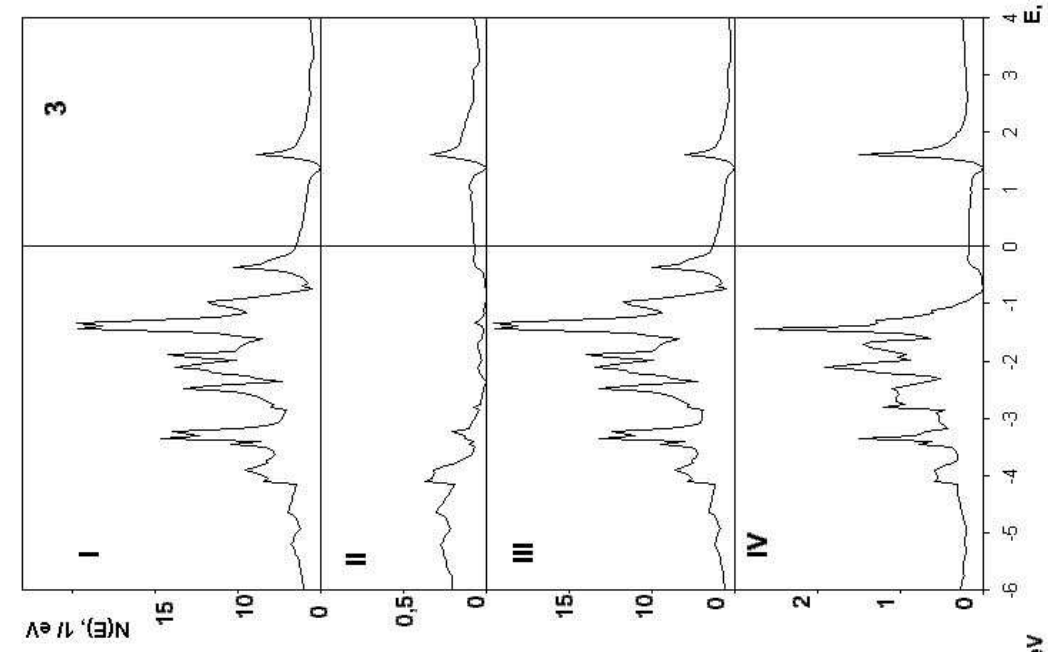
Fig.1. Energy bands 1 - MgCN₃, 2 - InBN₃, 3 - ScBN₃, 4 - MgCCu₃.

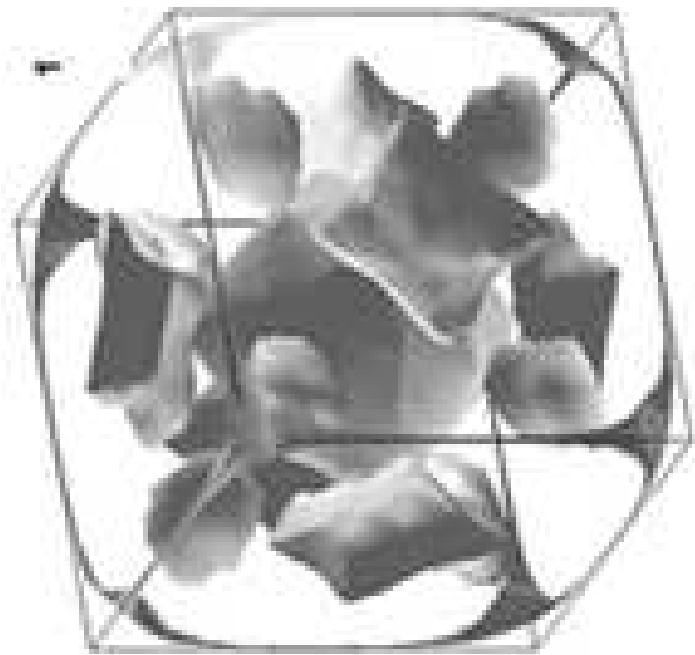
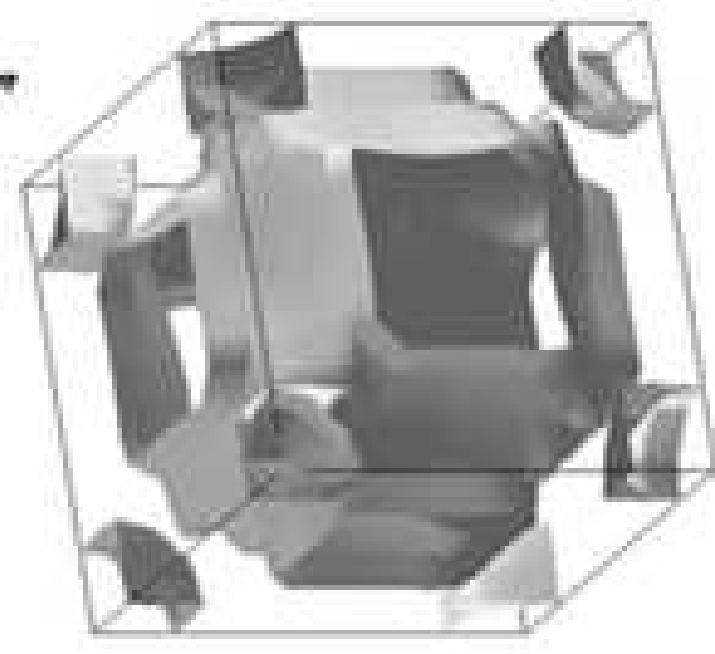
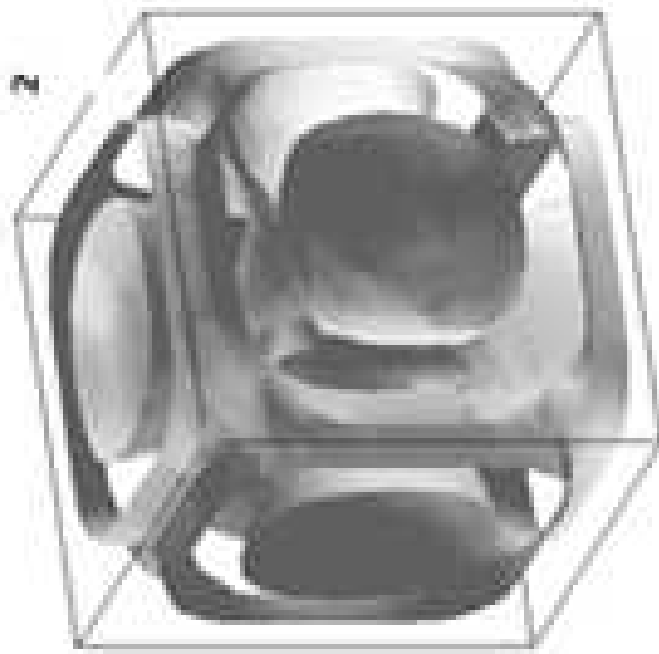
Fig.2. Density of state 1 - MgCN₃, 2 - ScBN₃, 3 - InBN₃ : I - Total DOS, II - atoms B, C DOS, III - atom N DOS, IV - atom Mg, Sc, In DOS

Fig.3. Fermi surfaces for: 1 - MgCN₃, 2 - InBN₃, 3 - ScBN₃, 4 - MgCCu₃.

Fig.4. Charge densities in 1 - MgCN₃ and 2 - ScBN₃ in 1/eV³.







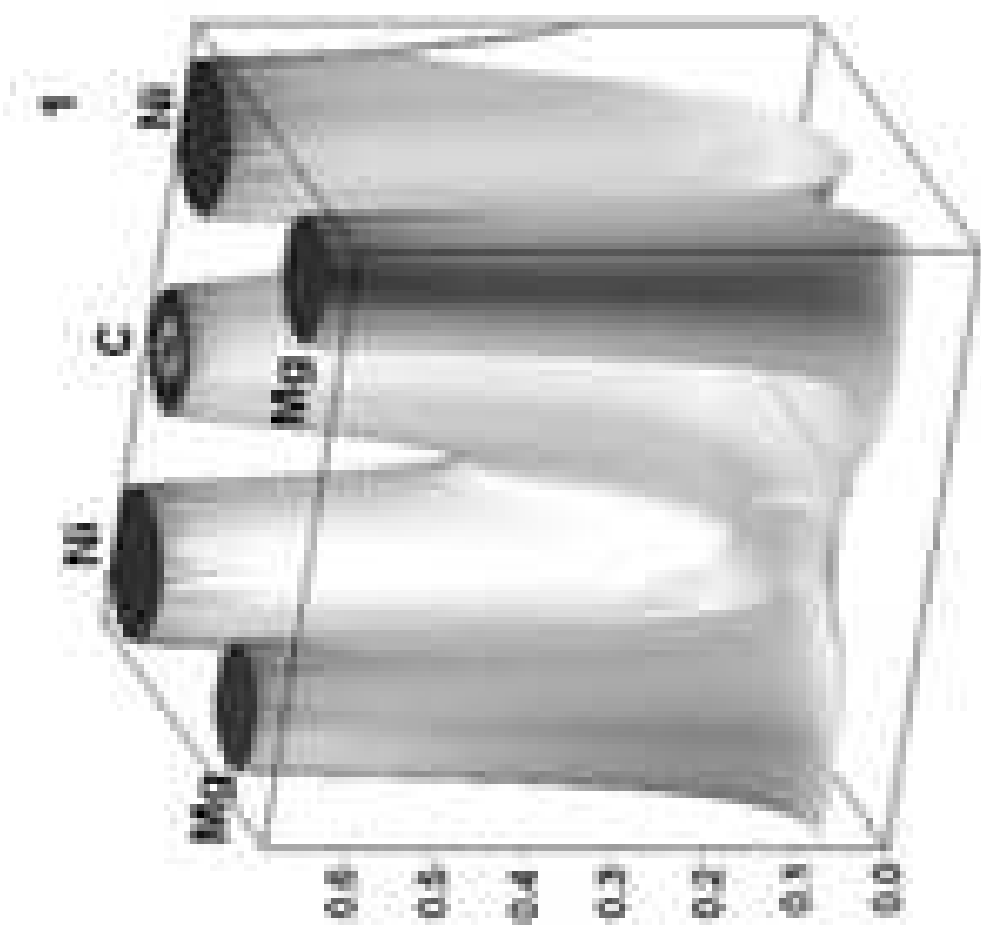
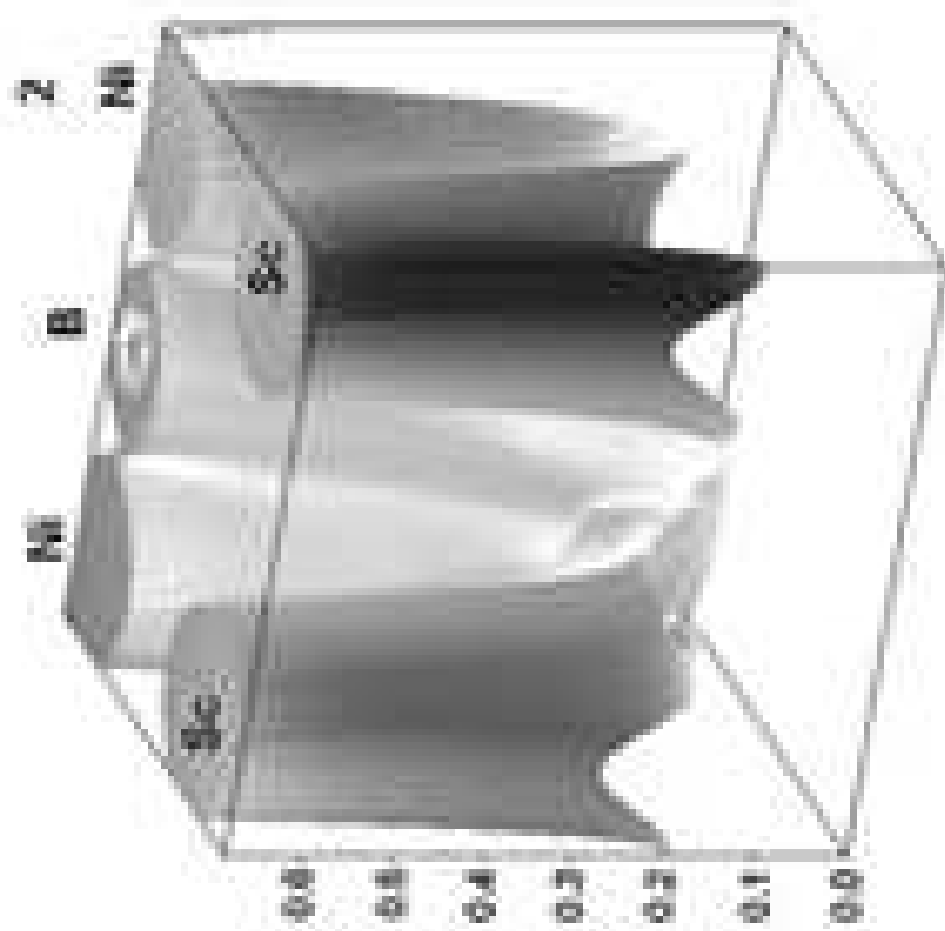


Table 1. Total and orbital DOS at the level ($N(E_F)$, $N_i(E_F)$, $1/\text{eV}$) for MgCNi_3 ets

MxM'_3	$N(E_F)$	M_s	M_p	M_d	X_s	X_p	M'_s	M'_p	M'_d
MgCNi_3	4,57	0,00	0,12	0,02	0,01	0,23	0,07	0,09	4,04
MgENi_3	2,38	0,04	0,04	0,04	0,02	0,00	0,02	0,06	2,16
MgCCo_3	2,41	0,01	0,01	0,03	0,00	0,01	0,00	0,01	2,33
MgCCu_3	0,38	0,04	0,06	0,03	0,00	0,03	0,02	0,04	0,17
ScBNi_3	2,59	0,00	0,11	0,20	0,00	0,11	0,05	0,09	2,03
InBNi_3	1,47	0,01	0,06	0,01	0,01	0,08	0,02	0,05	1,24